

A condensate storage ring

A. S. Arnold, C. S. Garvie, and E. Riis

Dept. of Physics, University of Strathclyde, Glasgow G4 0NG, UK

www.photonics.phys.strath.ac.uk

(Dated: December 2, 2024)

We experimentally investigate the behavior of cold atomic clouds and condensates released from the top of a vertically-oriented 10 cm diameter magnetic storage ring. The ring's atom number, vacuum lifetime and area are orders of magnitude larger than in previously reported experiments. As the initial atomic temperature is decreased, an increasingly large fraction of atoms is lost from the ring due to Majorana spin-flip transitions. We have 'plugged' this atomic leak by applying an adjustable azimuthal magnetic field. Without this field condensates vanish before one revolution, but with a 10G field multiple revolutions are possible with negligible atomic loss, in good agreement with a simple one-dimensional model.

The field of atom optics [1] has seen a plethora of significant advances since the advent of laser cooling [2] and gaseous Bose-Einstein condensation [3]. Analogs of mirrors, lenses, beamsplitters and waveguides for manipulating ultra-cold atoms now exist and are continually being improved. Alongside these developments the same basic magnetic and optic interactions have been used in the development of a number of atomic traps.

Much less attention has been directed to a hybrid between atom optical elements and traps, the cold atom storage ring, where atoms are guided around a closed path. This is an interesting configuration for performing, for instance, ultra-sensitive atom interferometry. An application of particular interest is rotation sensing, where the potential sensitivity increases with the enclosed area. An electrostatic storage ring was first reported for molecules [4] in 2001. However, for many interferometry experiments atoms are more suitable candidates as, in contrast to molecules, atoms are easily prepared in the same quantum state and they can be laser cooled to very low temperatures.

The first atomic storage ring made use of the interaction of a weak-field-seeking atom with the magnetic quadrupole field created by two concentric current carrying loops [5]. A stronger trapping field is obtained by using the quadrupole field created by the more symmetric four-wire geometry. This field configuration is the basis for our storage ring reported earlier [6]. A third group has recently developed a storage 'stadium' [7] based on a magnetic waveguide. Our ring contains more than 5×10^8 atoms, has a lifetime of 50 s and an area of 72 cm^2 . This corresponds to a relative increase of 100 (10), 60 (50) and 23 (7) in atom number, lifetime and area respectively, with respect to Ref. 5 (Ref. 7). The Sagnac effect [8] is linearly proportional to the area of an interferometer, and the area of our ring compares very favourably with the area of a state-of-the-art thermal beam atom interferometer gyro ($A = 0.22 \text{ cm}^2$ [9]). Additionally, since our ring has a long lifetime, the atoms can complete tens of revolutions, further increasing our effective area and thus the interferometric sensitivity.

In addition to the advantages in size and number the storage ring presented in this paper has the unique feature that we are able to form a Bose-Einstein condensate in a section of the ring [6]. This brings with it the potential to take advantage of the increased interferometric phase sensitivity afforded by using N -atom condensates ($\delta\phi_{BEC} \propto N^{-1}$) instead of N thermal atoms ($\delta\phi_T \propto N^{-1/2}$) [10].

We begin by considering the storage ring theoretically, before discussing our experimental setup. Comparisons will then be drawn between our experimental and theoretical results.

All magnetic atom-optical elements make use of the Stern-Gerlach potential $U = \mu_B g_F m_F B$ experienced by an atom moving adiabatically in a magnetic field of magnitude B , where μ_B is the Bohr magneton, m_F the atom's hyperfine magnetic quantum number, and g_F is the Landé g-factor. To make a storage ring one must use atoms in weak-field-seeking magnetic states ($g_F m_F > 0$), which are attracted to minima of the magnetic field magnitude. Using the Biot-Savart law, one can express the cylindrically symmetric magnetic field from a single coil of radius R , $\mathbf{b}_R(r, z)$, in terms of elliptic integrals [11]. Our storage ring comprises four concentric circular coils, with a toroidal quadrupole total magnetic field:

$$\begin{aligned} \mathbf{B}(r, z) = & \mathbf{b}_{R-\delta_R}(r, z - \delta_z) - \mathbf{b}_{R-\delta_R}(r, z + \delta_z) \\ & - \mathbf{b}_{R+\delta_R}(r, z - \delta_z) + \mathbf{b}_{R+\delta_R}(r, z + \delta_z). \end{aligned} \quad (1)$$

In our experiment $R = 5.0 \text{ cm}$, $\delta_R = 1.25 \text{ cm}$, and $\delta_z = 1.35 \text{ cm}$, leading to a ring of zero magnetic field at a radius $R_0 = 4.8 \text{ cm}$ slightly smaller than the mean coil radius R .

The theory of the storage ring for cold atoms is relatively simple, as the spatio-temporal evolution of each atom can be accurately described using the equations of motion arising from the Stern-Gerlach potential. After choosing suitable Gaussian initial position and velocity distributions it is possible to perform a Monte Carlo simulation to build up a spatio-temporal atomic density map.

By comparison with a 3D model, we have found that a 1D model is sufficient, i.e. the rigid pendulum equation:

$$\frac{d^2\theta}{dt^2} \left(= \frac{d\omega}{dt} = \omega \frac{d\omega}{d\theta} \right) = \frac{g \sin \theta}{R_0}, \quad (2)$$

where θ and $\omega = \frac{d\theta}{dt}$ are the angular position and velocity of an atom, g is the acceleration due to gravity and R_0 is the radius of the storage ring. Note that Eq. 2 can be integrated analytically, given the initial angle (θ_0) and angular velocity (ω_0) of an atom, to determine the time-averaged relative probability of finding an atom at a given angle:

$$P(\theta) \propto \frac{1}{\omega(\theta)} = \frac{dt}{d\theta} = \left(\omega_0^2 + \frac{2g}{R_0} (\cos \theta_0 - \cos \theta) \right)^{-1/2}. \quad (3)$$

In our vertically-oriented storage ring there is therefore a high time-averaged probability of finding atoms in the region where they travel the slowest – the top of the ring. The integral of Eq. 3, leads to an expression for $t(\theta)$ in terms of an elliptic integral. There are two kinds of trajectories in the ring (Fig. 1): if $\cos(\theta_{max}) = |\frac{R_0}{2g}\omega_0^2 + \cos \theta_0| > 1$ an atom will always rotate in the same direction, but if $\cos(\theta_{max}) \leq 1$ the atom will reverse its direction around the ring at the turning points $\theta = \pm\theta_{max}$.

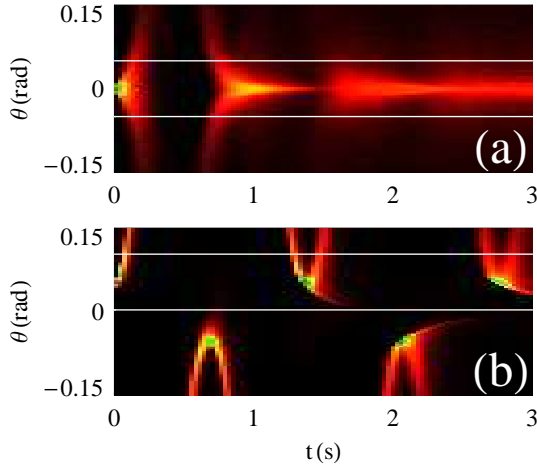


FIG. 1: (Color online) A Monte-Carlo simulation of atomic dynamics in the vertically-oriented storage ring for a $2\mu\text{K}$ initial cloud of atoms. Images (a) and (b) represent lossless atom dynamics for a cloud released at $\theta = 0$ and $\theta = 60$ mrad respectively. The white lines mark the extent of our 110 mrad experimental viewing region.

The theoretical time-dependent angular distribution of atoms can be seen in Fig. 1. An atomic cloud in a parabolic potential can expand or shrink, but will maintain the same cloud shape. A circular atomic trajectory has a potential which is only parabolic to second order, and it is the higher order effects which cause an atomic

cloud released from the top of the ring ($\theta=0$) to break into two halves (Fig. 1(a)), leaving a near-zero probability at the top of the ring after around 300 ms. These two halves return to the top of the ring after a further 300 ms and have a non-zero probability of remaining at the top of the ring for all subsequent times. The time for the two halves of the atomic cloud to ‘recombine’ has only a weak dependence on the initial atomic temperature. Gravity is the dominant effect for cold atoms, leading to a ‘hot’ velocity of 1.4 m s^{-1} at the bottom of the ring – a good location for future studies of high-energy collisions between BECs.

Note that although the spread of initial thermal velocities quickly ensures that atoms reach the top of the ring at different times, in Fig. 1 we still see slowly decaying ‘echos’ of the originally localised spatial atomic cloud in the form of time-varying bimodal perturbations of the θ distribution. The angular width of these echos is approximately proportional to the initial cloud width, so the echos and their bimodal nature become more pronounced at higher temperatures.

We now turn to the experimental setup, for which many of the details are in Refs. [6, 12]. Our double magneto-optical trap (MOT) [13] collects more than 10^9 ^{87}Rb atoms in both our high and low pressure MOT chambers. The storage ring (Fig. 2) can be loaded directly from the low pressure MOT or Ioffe-Pritchard (IP [14]) trap without the need for any additional magnetic guiding or transfer, i.e. the MOT and IP trap are at the top of the ring.

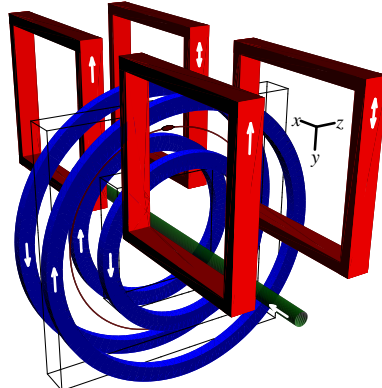


FIG. 2: (Color online) The storage ring/MOT/IP magnetic coils. Four circular coils (blue) with average diameter 10 cm make up the storage ring (thin red circle) to which the axial wire (green) can add an adjustable azimuthal magnetic field. The two pairs of square coils (red) can localise the atoms (red cigar) at the top of the ring in either a MOT or IP trap depending on the current direction in the right coil pair. The black lines indicate the edges of the quartz vacuum chamber. The large coil sizes ensure good optical access, and low magnetic field noise. Absorption imaging is along the x axis and gravity is in the y direction.

The advantage of our hybrid magnetic trap is that,

using the same coils, it can be (i) a MOT, (ii) an IP magnetic trap (with trap frequencies $\nu_r = 230$ Hz, $\nu_z = 10$ Hz) or iii) a toroidal magnetic storage ring with radial gradient 230 G/cm. In modes (i) and (ii) the magnetic field has an adjustable aspect ratio in the azimuthal direction. The four 2 turn $\times 500$ A circular coils in Fig. 2 create a toroidal magnetic quadrupole field, confining the atoms to a ring. The four 3 turn $\times 500$ A square pinch coils are wired in pairs, and confine the atoms to a localised section of the ring for Ioffe-Pritchard trapping of the atoms. If the direction of one of the pinch coil pairs is reversed a 3D quadrupole field can be generated for operating the MOT.

After loading the low pressure MOT, the atomic cloud is optically pumped, loaded into the IP trap, magnetically compressed, and then evaporatively cooled to an adjustable temperature. The atoms can then be smoothly loaded into the storage ring in 20 ms. Since 2003 we have been able to form Bose-Einstein condensates containing $N_0 = 2 \times 10^5$ atoms at the top of the storage ring [6] at a typical final RF evaporation frequency of 740 kHz.

In order to compare our experimental ring data with our theoretical model, we have found it convenient to model the total number of atoms in the ‘viewing window’ of our absorption imaging system as a function of time. Our CCD camera has an area of 4.8×6.4 mm 2 , with a magnification of 1.20(1). We have released cold atomic clouds with three different final evaporation temperatures into a storage ring with no azimuthal field, namely: $T = 350 \mu\text{K}$, $50 \mu\text{K}$ and $2 \mu\text{K}$. In accordance with theory,

the atoms disappear after 400 ms, reappear shortly afterwards, and are present at all subsequent times. However as the atomic samples get colder, there is a marked decrease in the fraction of visible atoms as a function of time. Although the atoms experience the same vacuum conditions, the colder atomic clouds decay from the ring at a much faster rate.

The marked variation in the storage ring dynamics with atomic cloud release temperature can be explained in terms of non-adiabatic Majorana spin-flip transitions [15]. In the storage ring we have a toroidal quadrupole magnetic field which has a ring of zero magnetic field. Atoms with colder temperatures pass closer to the magnetic field zero, and are therefore selectively removed from the storage ring. If we apply a constant magnetic field across the entire storage ring, perpendicular to the ring axis, it is possible to have only two places in the ring with zero magnetic field, however there will be a strong angular variation in the trapping potential.

A novel feature of our storage ring is that the ‘hole’ in our quartz vacuum chamber (Fig. 2) allows us to use a wire along the axis of the storage ring. This means that we can generate an azimuthal magnetic bias field $B_\theta = 0\text{--}10$ G around the ring which transforms the radial magnetic potential from a cone to a hyperbola. Atom loss is therefore stopped as the toroidal quadrupole’s ring of zero magnetic field is removed and Majorana transitions are drastically reduced. The dramatic difference that the azimuthal field makes can be seen in Figs. 3,4.

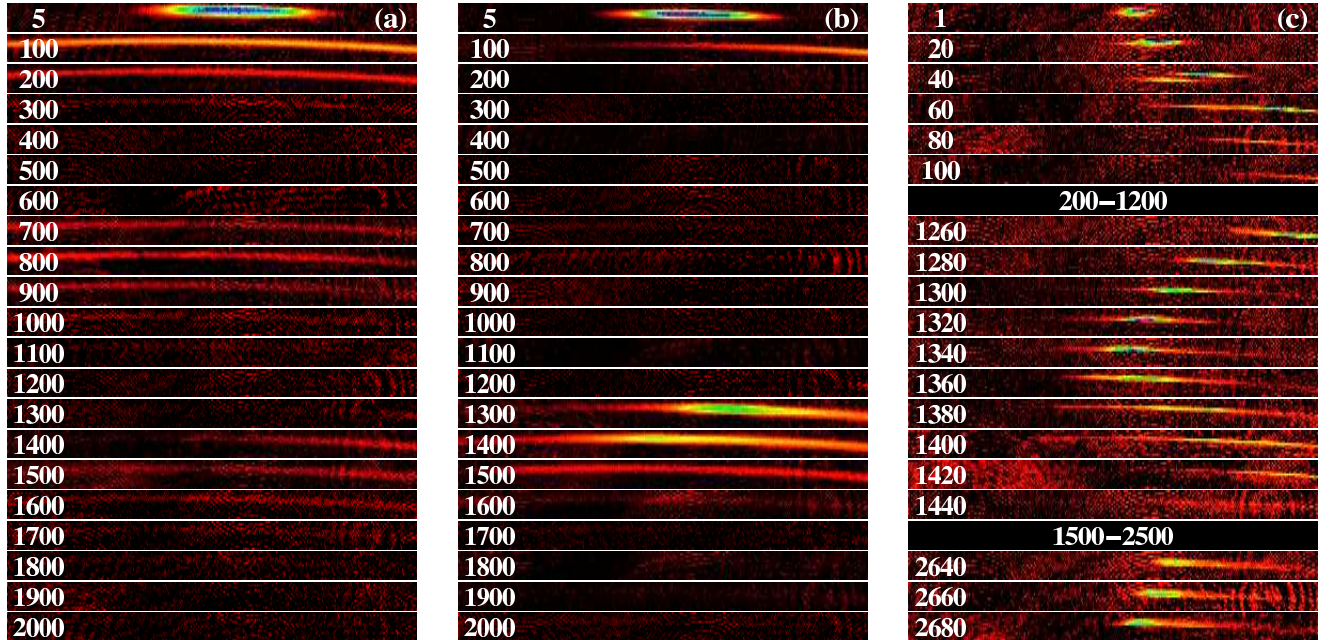


FIG. 3: (Color online) Storage ring dynamics for $2 \mu\text{K}$ atoms with (a) $B_\theta = 0$ G and (b) $B_\theta = 10$ G (middle) – numbers denote time in ms. In (c) multiple revolutions of a BEC in a ring with $B_\theta = 10$ G are seen. Atoms/BECs in (b)/(c) are launched away from the top of the ring (i.e. $\theta_0 \neq 0$) to enable refocusing. Absorption images are 0.4×5.4 mm 2 .

Note that when we performed experiments with an azimuthal field, the atoms/BECs were not launched from $\theta_0 = 0$. If atoms are launched from $\theta_0 = 0$ (Fig. 1(a)), then although the total number of atoms observed (Fig. 4) is similar to the $\theta_0 \neq 0$ case, the size of the returning $\theta_0 \neq 0$ cloud is much smaller and clearer due to focusing in the ring (Figs. 1(b), 3(b,c)).

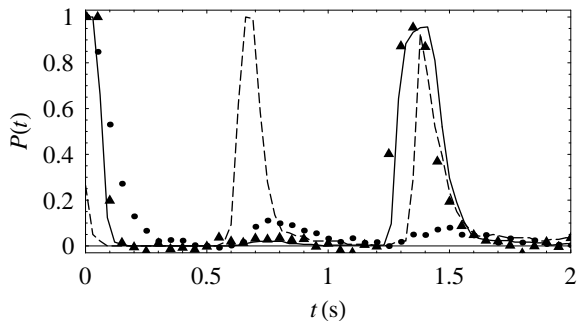


FIG. 4: The relative atomic population, $P(t)$, viewed by the CCD camera as a function of time for $2 \mu\text{K}$ atoms. Experimental data with $B_\theta = 0 \text{ G}$ and $B_\theta = 10 \text{ G}$ are shown with circles and triangles respectively. The relative Monte Carlo atomic population in the viewing region of Fig. 1(a) (dashed curve) and Fig. 1(b) (solid curve) are shown for comparison. Good quantitative agreement can be seen between the $B_\theta = 10 \text{ G}$ data and the Monte Carlo simulation of an atomic cloud released from $\theta_0 = 60 \text{ mrad}$. Due to large Majorana losses the $B_\theta = 0 \text{ G}$ data does not fit either of the theoretical curves.

We have not seen, nor do we expect to see, phase-fluctuations [17] in our condensate before or after propagation in the ring. These effects have been studied in highly elongated condensates in which the BEC coherence length is less than the length of the condensate. We form the condensate in only a moderately elongated trap, and the azimuthal expansion process is rapid enough that the (density-dependent) phase fluctuations do not have time to develop.

Sagnac interferometry will be performed by locating the condensate at the exact top of the ring, and incoherently splitting the sample by simply releasing them into the ring and looking for interference fringes after a single revolution. Coherent splitting of the BEC will be achieved using Bragg scattering [18] to send BEC wavepackets in both directions around the ring. Although interferometry can be performed using cold atoms, the minimum detectable phase shift decreases from $(\delta\phi \approx 1/\sqrt{N})$ to $(\delta\phi \approx 1/N)$ when BECs (coherent atoms) are used and we aim to enter this regime.

In conclusion, we have demonstrated a 10 cm diameter storage ring for cold ^{87}Rb atomic clouds and BECs. The atoms are released from an IP magnetic trap, and the release temperature can be tuned via evaporative cool-

ing. By including an azimuthal bias field around the ring Majorana losses were prevented and low-loss BEC propagation is now possible within the ring. The condensate has made at least 6 revolutions around the ring, travelling distances of nearly 2 m . Our goal is a highly sensitive Sagnac atom interferometer, in which we are aided by our unprecedented ring area.

We would also like to point out that if one cannot create an azimuthal magnetic field, it is still possible to prevent spin-flip losses by using an adjustable-radius time-orbiting ring trap (TORT) [16]. As we were finishing our own Letter we learnt that a team in Berkeley has very recently created the first TORT for BECs [19]. Their condensate population and lifetime is similar to our own, but the area of their ring is 0.05 cm^2 .

We are grateful for helpful discussions with K. Burnett. This work was supported by the UK EPSRC and the University of Strathclyde.

- [1] C. S. Adams and E. Riis, *Prog. Quant. Electr.* **21**, 1 (1997); E. A. Hinds and I. G. Hughes, *J. Phys. D* **32**, R119 (1999).
- [2] S. Chu *et al.*, *Phys. Rev. Lett.* **55**, 48 (1985); E. L. Raab *et al.*, *Phys. Rev. Lett.* **59**, 2631 (1987).
- [3] M. H. Anderson *et al.*, *Science* **269**, 198 (1995); K. B. Davis *et al.*, *Phys. Rev. Lett.* **75**, 3969 (1995); C. C. Bradley *et al.*, *Phys. Rev. Lett.* **79**, 1170 (1997).
- [4] F. M. H. Crompvoets *et al.*, *Nature* **411**, 174 (2001).
- [5] J. A. Sauer, M. D. Barrett, and M. S. Chapman, *Phys. Rev. Lett.* **87**, 270401 (2001).
- [6] C. S. Garvie, E. Riis and A. S. Arnold, *Laser Spectroscopy XVI*, P. Hannaford *et al.* eds., p178 (World Scientific, Singapore, 2004); see also www.photonics.phys.strath.ac.uk.
- [7] S. Wu *et al.*, *Phys. Rev. A* **70**, 013409 (2004).
- [8] M.G. Sagnac, *C.R. Acad. Sci.* **157**, 708 (1913).
- [9] T. L. Gustavson, P. Bouyer and M. A. Kasevich, *Phys. Rev. Lett.* **78**, 2046 (1997).
- [10] J. Jacobson, G. Bjork and Y. Yamamoto, *Appl. Phys. B* **60**, 187 (1995).
- [11] R. H. Good, *Eur. J. Phys.* **22**, 119 (2001).
- [12] A. S. Arnold and E. Riis, *J. Mod. Opt.* **49**, 959-964 (2002).
- [13] K. Gibble, S. Chang and R. Legere, *Phys. Rev. Lett.* **75**, 2666 (1995); C. J. Myatt *et al.*, *Opt. Lett.* **21**, 290 (1996).
- [14] D.E. Pritchard, *Phys. Rev. Lett.* **51**, 1336 (1983).
- [15] W. Petrich *et al.*, *Phys. Rev. Lett.* **74**, 3352 (1995).
- [16] A.S. Arnold, *J. Phys. B* **37**, L29 (2004).
- [17] D.S. Petrov, G.V. Shlyapnikov and J.T.M. Walraven, *Phys. Rev. Lett.* **87**, 050404 (2001); S. Dettmer *et al.*, *ibid.* **87**, 160406 (2001); D. Hellweg *et al.*, *ibid.* **91**, 010406 (2003); S. Richard *et al.*, *ibid.* **91**, 010405 (2003).
- [18] J. Stenger *et al.*, *Phys. Rev. Lett.* **82**, 4569 (1999); M. Kozuma *et al.*, *Phys. Rev. Lett.* **82**, 871 (1999).
- [19] S. Gupta *et al.*, cond-mat/0504749, submitted to PRL.